Supplementary Figure 1

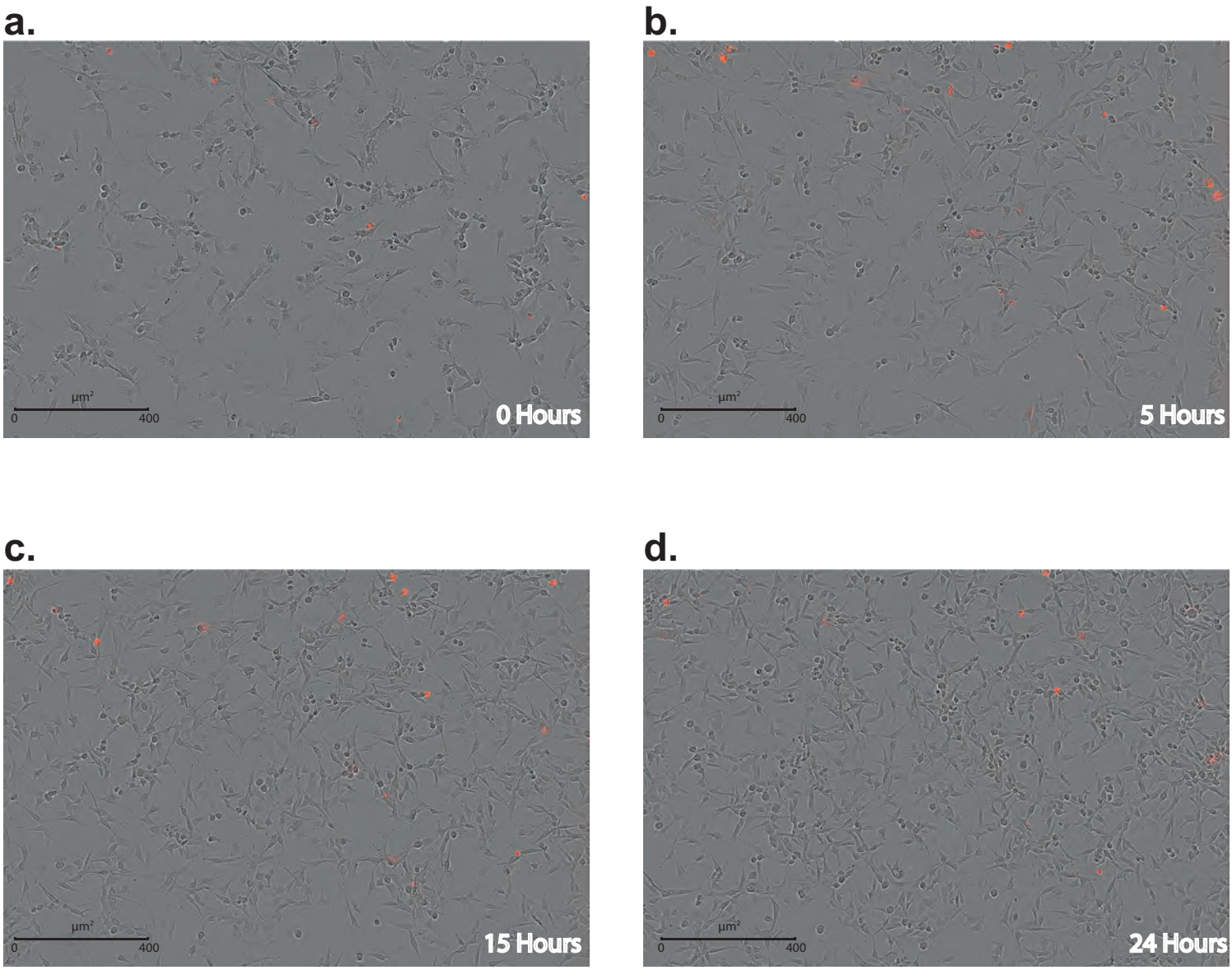

Supplementary Figure 1: U87-EGFRvIII cells retain morphology with minimal cell death after culturing in murine T cell media. Cultures of human U87-EGFRvIII cells in mouse T cell media were established and imaged using a live cell imaging IncuCyte assay over the course of 24 hours as a control for functional assays, in the presence of propidium iodide (PI). The U87-EGFRvIII cells retain morphology at the later time points with minimal PI signal (indicative of cell death). Hours indicates time in culture after media change. Cultures were established in triplicate. Shown is one representative image.
The scale bar is 400 μM.

Supplementary Figure 2

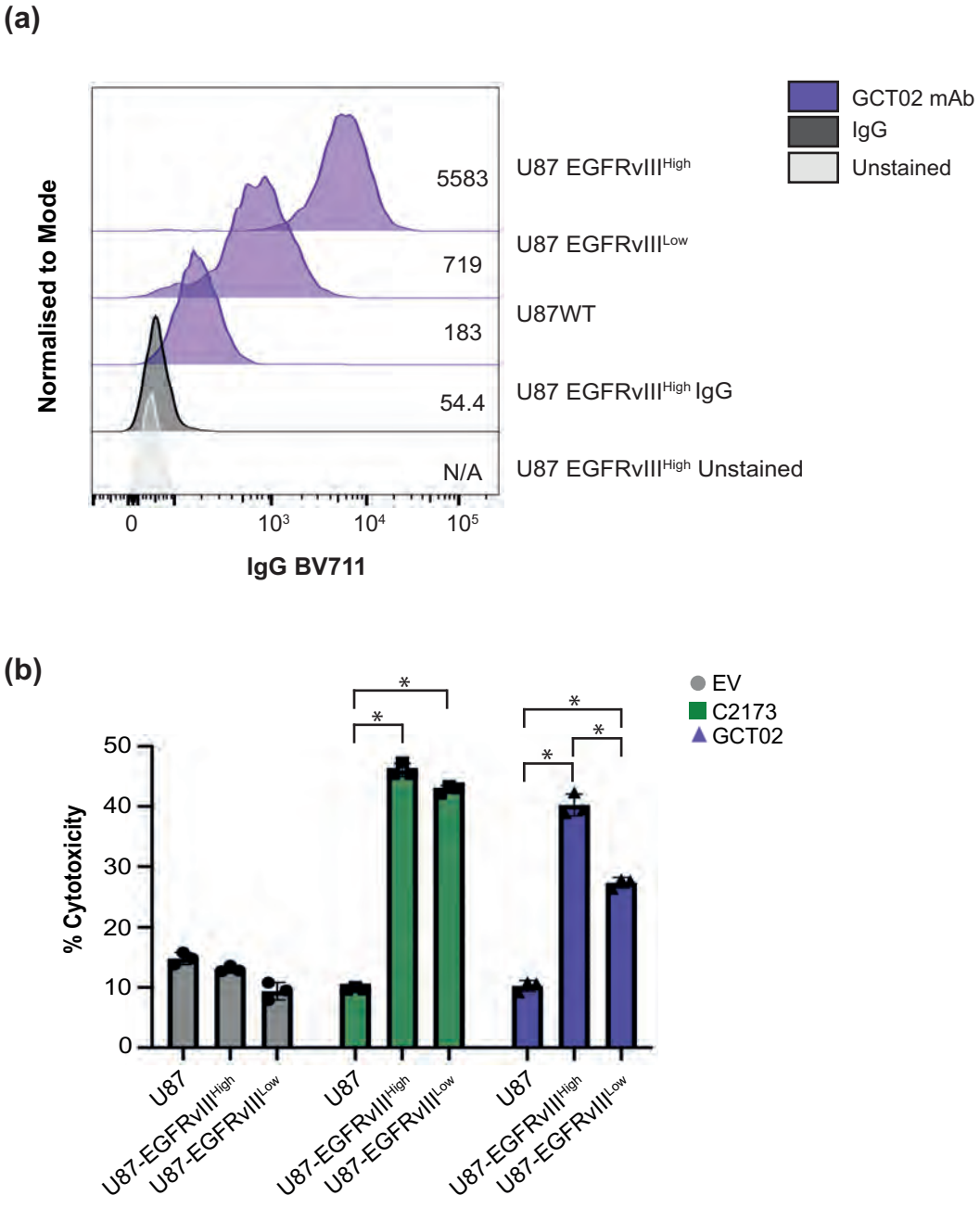

Supplementary Figure 2. CD8⁺ GCT02 CAR T cells show reduced efficacy against EGFRvIII low cell line in vitro.
(a) Flow cytometry analysis of U87, U87-EGFRvIIIHigh and U87-EGFRvIIILow labelled with the GCT02 monoclonal antibody.
(b) Cytotoxicity induced by CD8⁺ GCT02 and C2173 CAR T cells coincubated with panel of chromium-labelled human glioblastoma cell lines; U87, U87-EGFRvIII^{High} or U87-EGFRvIII^{Low} for 24 hours.
Data shows mean±SD, n=3 technical replicates and are representative of 3 experiments. Statistical analysis was determined by the one-way ANOVA, Multiple comparisons. * *P*-value <0.05.

Supplementary Figure 3

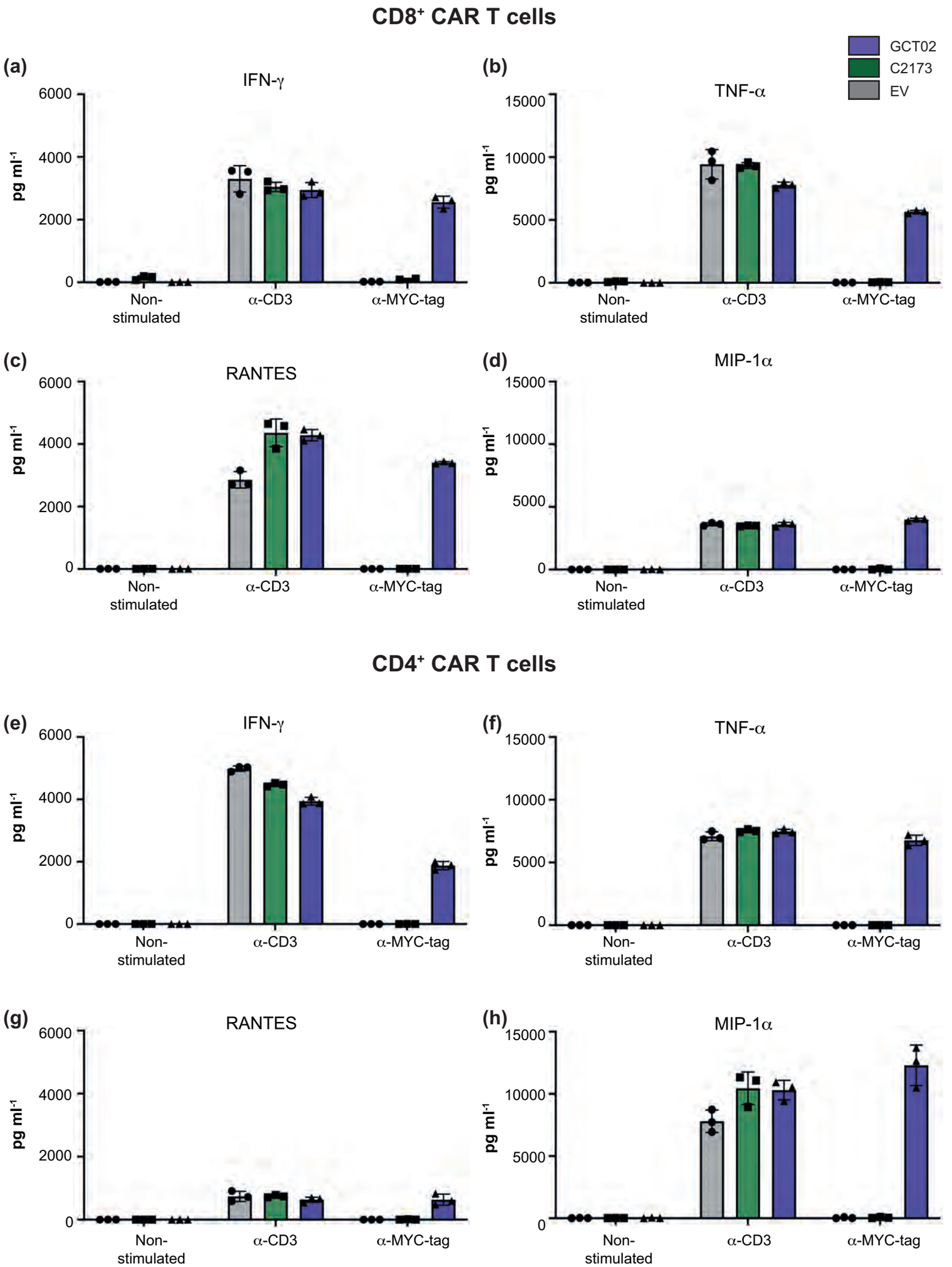

Supplementary Figure 3 GCT02 CAR T cells produce cytokine in response to anti-Tag stimulation. Cytokine bead array quantitation after 24 hours as assayed from cultures of purified **(a)** $CD8^+$ or (b) $CD4^+$ CAR T cells that were activated by either agonistic plate-bound anti-CD3 antibody as a maximum control or plate bound anti-MYC-tag. Shown is the secreted amount of IFN-γ, TNF-α, RANTES and MIP-1α in pg mL^{-1} of culture. Data shows mean±SD, n=3 technical replicates and are representative of 4 experiments.

Supplementary Figure 4

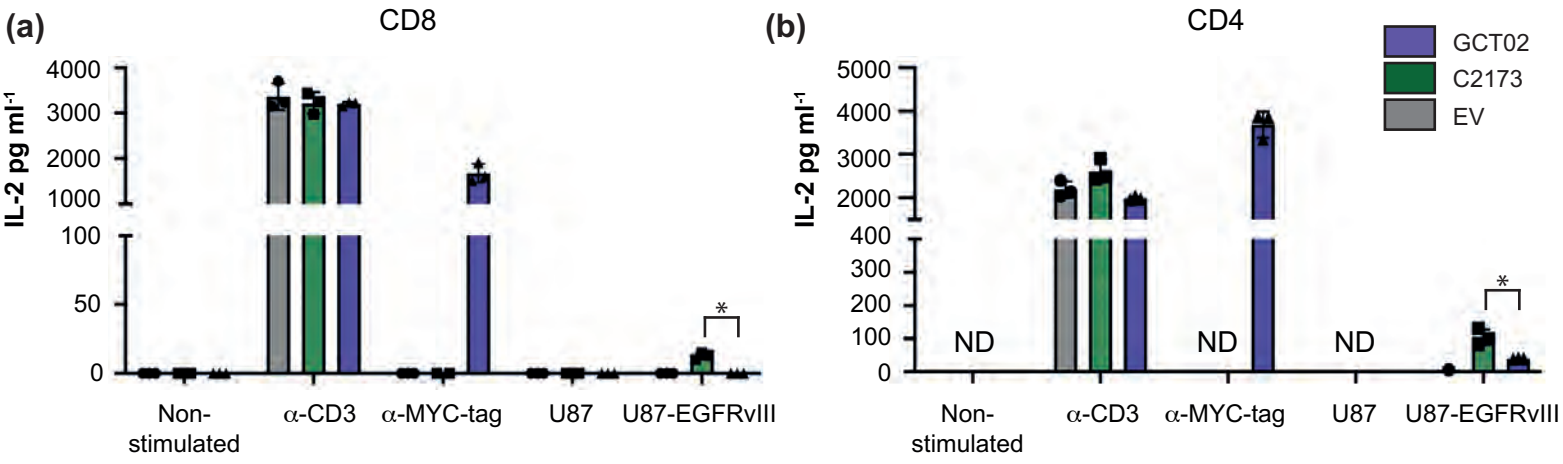

Supplementary Figure 4. Murine GCT02 CAR T cells do not produce IL-2 in response to U87-EGFRvIII stimulation. Cytokine bead array quantitation after 24 hours as assayed from cultures of purified **(a)** $CD8^+$ or **(b)** $CD4^+$ CAR T cells that were activated by either agonistic plate-bound anti-CD3 antibody as a maximum control, plate bound anti-MYC-tag, or co-cultured with U87, or U87-EGFRvIII target cells. Shown is the secreted amount of IL-2 in pg mL^{-1} of culture. Data shows mean±SD, n=3 technical replicates and are representative of 3 $CD8^+$ and 2 $CD4^+$ experiments. Statistical analysis was determined by the paired *t*-test. * *P*-value <0.05.

Supplementary Figure 5

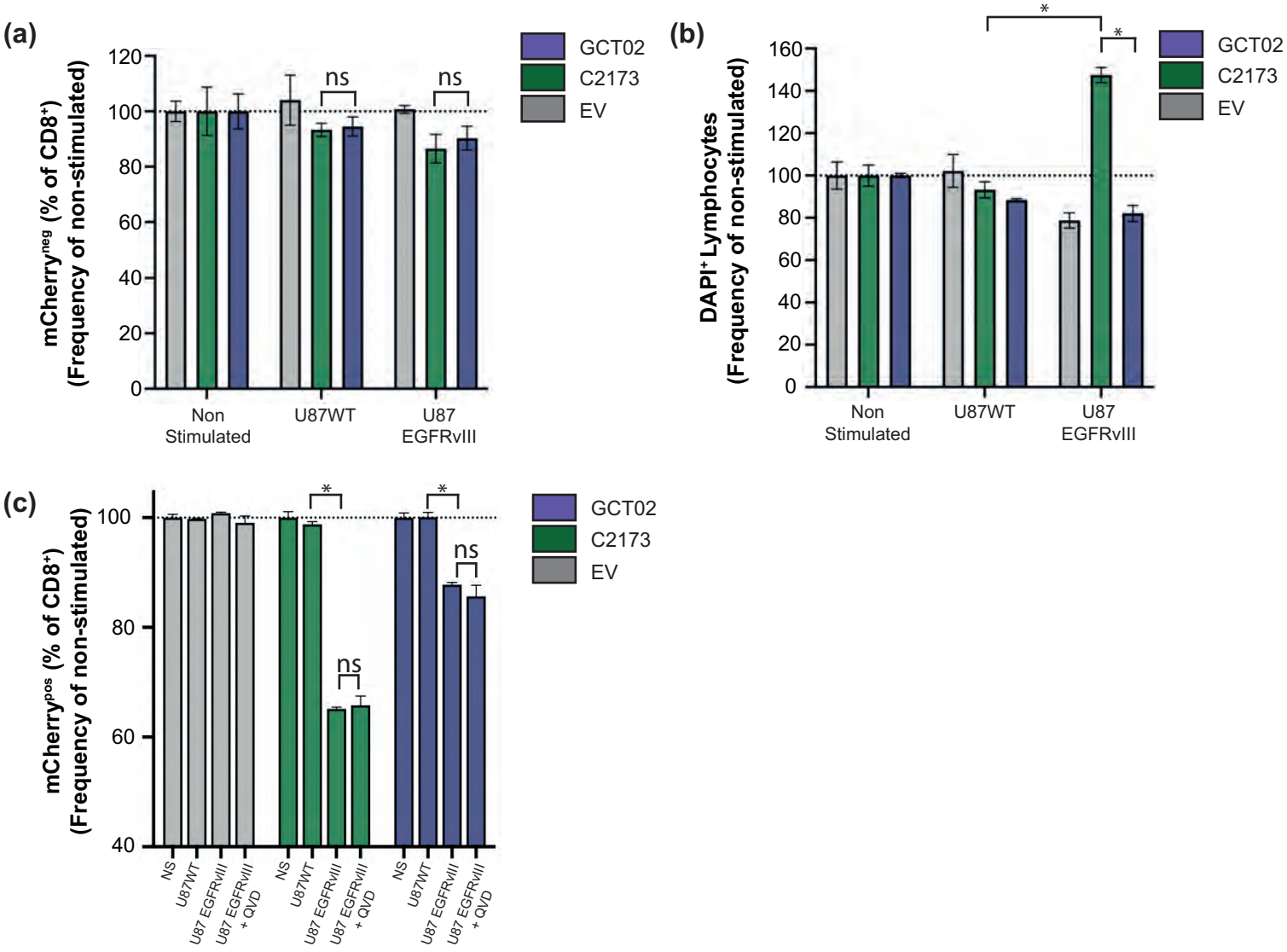

Supplementary Figure 5. CD8⁺ GCT02 CAR T cells show decreased cell death compared to C2173 CAR T cells upon exposure to U87-EGFRvIII cells.

(a) The relative number of mCherry^{neg}/CD8^{+} lymphocytes after 16 hours with either no stimulation (NS) (media alone), or coculture with U87 or U87-EGFRvIII cells. mCherry^{neg}/CD8^{+} event number in each sample was normalised to give mCherry^{neg}/CD8^{+} event count per 1 x 10^4 counting beads. Bars show mCherry^{neg}/CD8^{+} event count expressed as a percentage of the mean of non-stimulated conditions for each T cell group. Data shows mean±SD, n=3 replicates and are representative of 3 experiments. Statistical analysis was determined by the unpaired *t*-test, * *P*-value <0.05.

(b) The relative number of DAPI^{+}/CD8^{+} lymphocytes after 16 hours with either no stimulation (NS) (media alone), or coculture with U87 or U87-EGFRvIII cells. DAPI^{+}/CD8^{+} event number in each sample was normalised to give DAPI^{+} event count per 1 x 10^4 counting beads. Bars show DAPI^{+} event count expressed as a percentage of the mean of non-stimulated conditions for each T cell group. Data shows mean±SD, n=3 replicates and are representative of 3 experiments. Statistical analysis was determined by the unpaired *t*-test, * *P*-value <0.05.

(c) The percentage of mCherry^{pos}/CD8^{+} T cells remaining after 16 hours with either NS (media alone), or with coculture with U87 or U87-EGFRvIII cells ± QVD. Each sample was normalised by expression as a percentage of the mean NS frequency for each T cell group. Data shows mean±SD, n=3 replicates and are representative of 3 experiments. Statistical analysis was determined by the unpaired *t*-test, * *P*-value <0.05.

Supplementary Figure 6

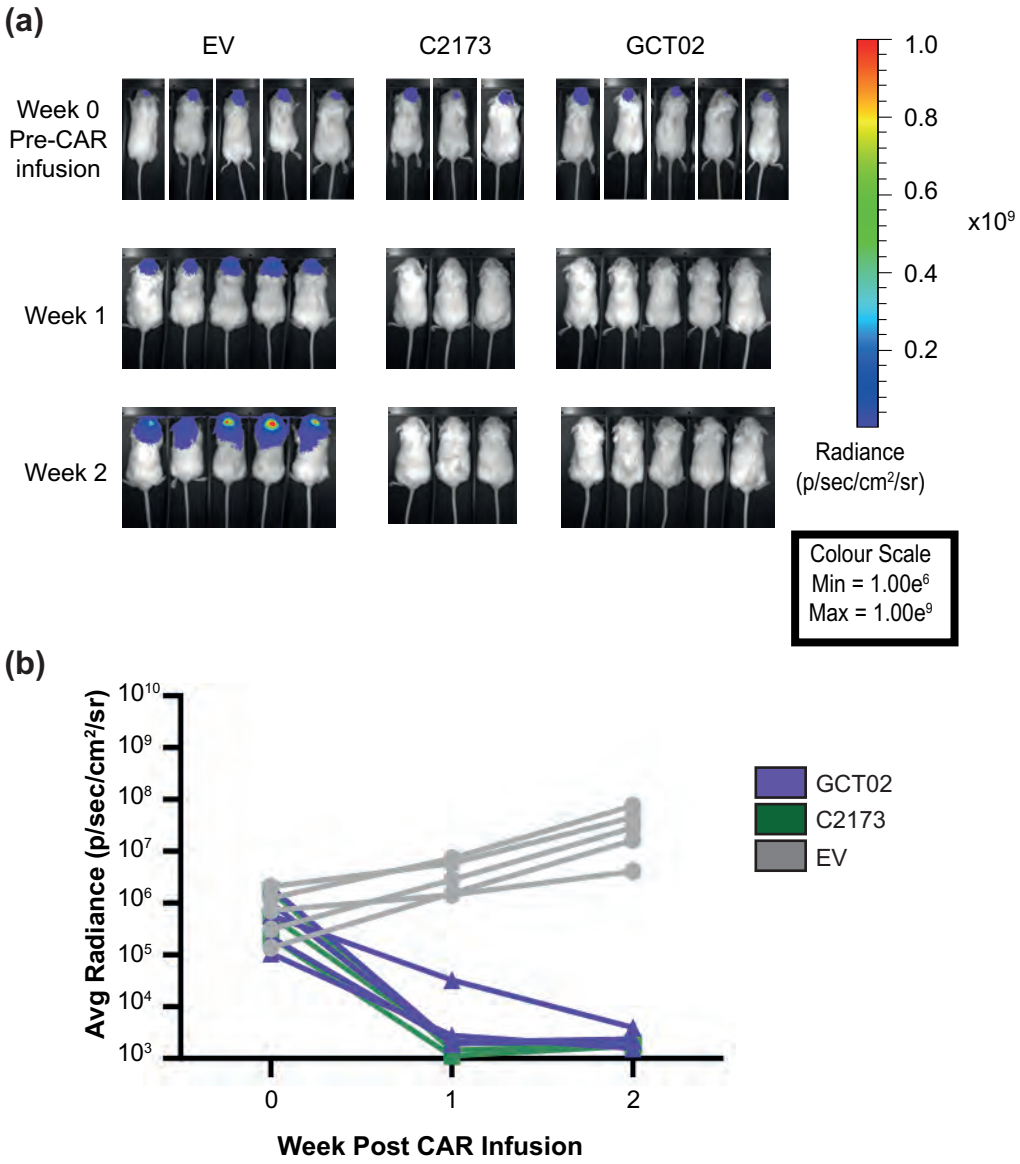

Supplementary Figure 6. GCT02 and C2173 CAR T cells mediate rapid regression of U87-EGFRvIIIns expressing tumours in vivo.
The second biological replicate of tumour regression induced by GCT02 and C2173 CAR T cells in vivo. **(a)** Bioluminescence imaging of U87-EGFRvIII-GFP-Luc tumour bearing NSG mice, treated with either empty vector (EV), C2173, or GCT02 CAR T cells. Individual mice from each treatment group are shown for up to 2 weeks after CAR T cell infusion. Representative of two independent experiments. **(b)** Quantification of tumour growth in the mice in panel (a). Tumour size was quantitated in radiance (photons/sec/area/sr). Each line represents a single mouse. n=5 mice per group for EV and GCT02 n=3 mice per group for C2173.

Supplementary Figure 7

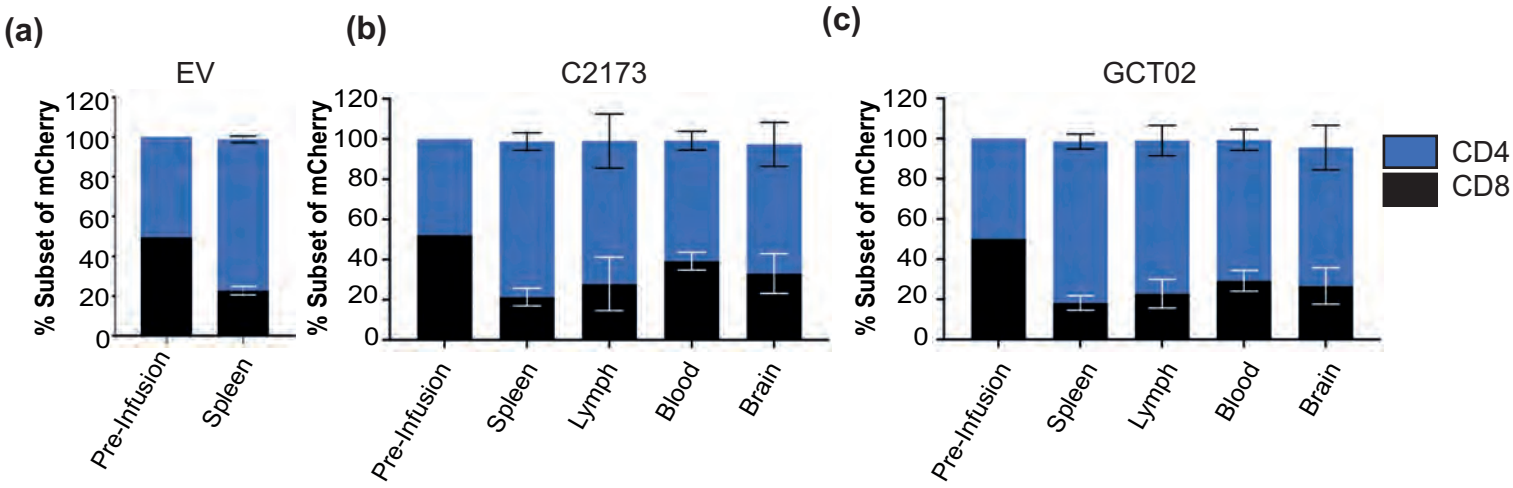

Supplementary Figure 7. Identified T cells are skewed towards CD4+ post in vivo infusion. Quantitated flow cytometric analysis of the CAR T treated mice, 19 days post infusion with CAR T cells. Data shows the proportion of $CD4^+$ to $CD8^+$ T cells in the spleen, compared to pre-infusion for the EV treated mice **(a)**, and in the spleen, lymph node, blood and brain compared to pre-infusion, in the **(b)** C2173 and **(c)** GCT02 mice. Cytometry data was gated on $CD3^+$ T cells and shown is the percentage $mCherry^+$ CAR T cells of the CD3+ population, for both $CD4^+$ (blue) and $CD8^+$(black) T cells. Shown is mean ± SD, n=3 to 5 mice. Representative of two independent biological replicates.

Supplementary Figure 8

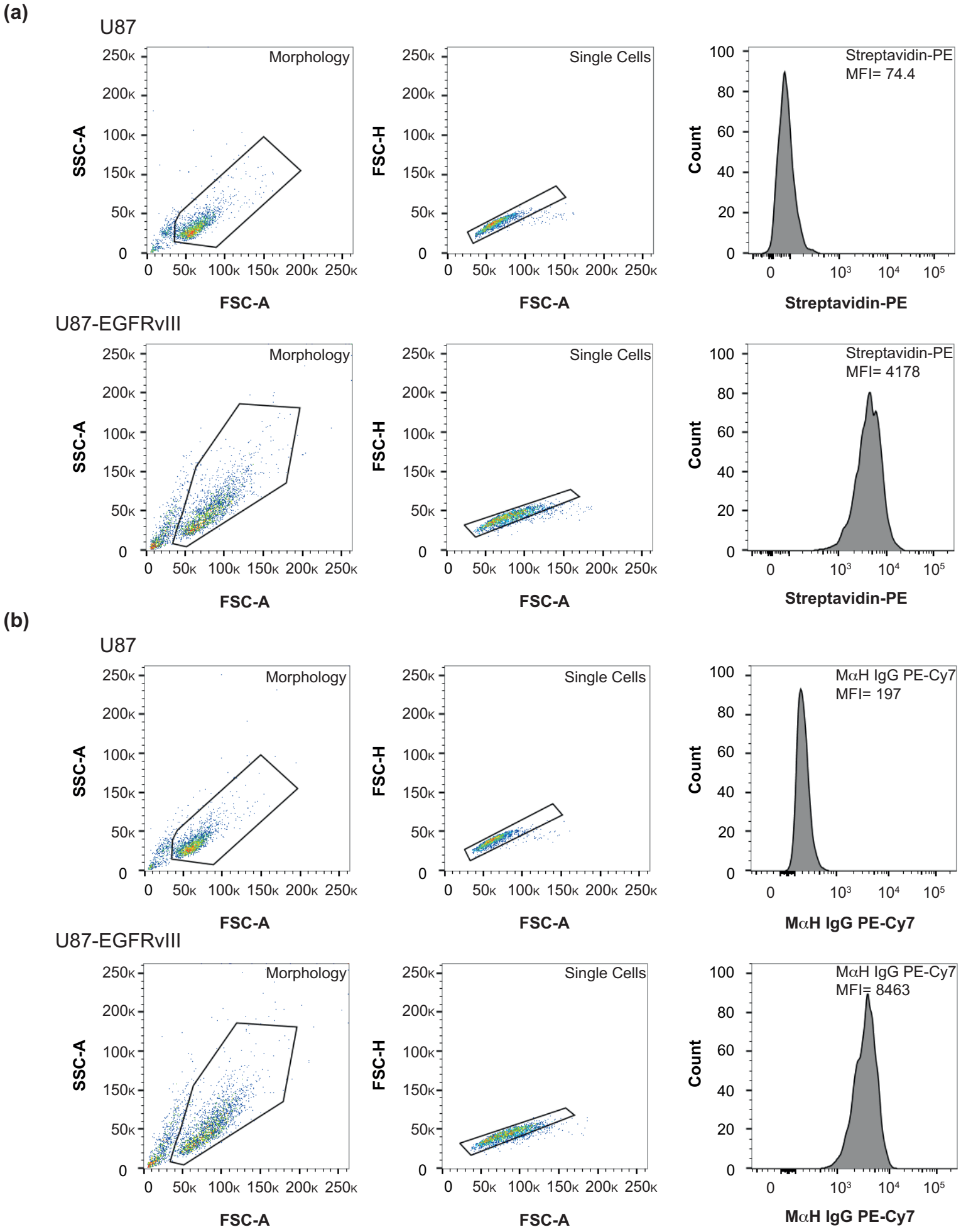

Supplementary Figure 8. Flow cytometry gating strategy for Figure 1.
(a) Flow cytometry gating strategy of U87 (top) and U87-EGFRvIII (bottom) to determine level of GCT02 scFv binding.
(b) Flow cytometry gating strategy of U87 (top) and U87-EGFRvIII (low) to determine level of Cetuximab scFv binding. Data are representative of 3 experiments.

Supplementary Figure 9

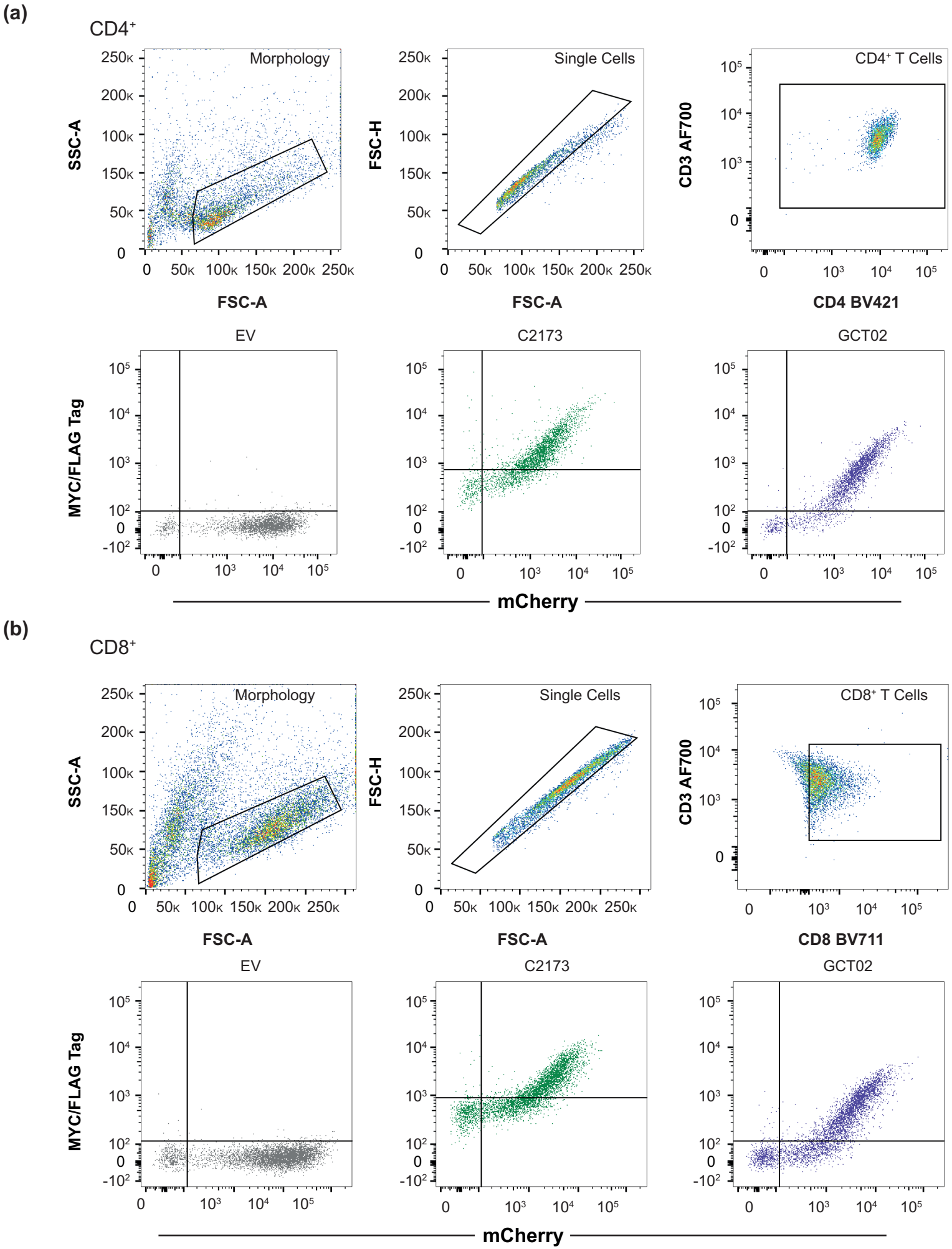

Supplementary Figure 9. Flow cytometry gating strategy for Figure 2b-d.
Flow cytometry analysis of (a) CD4+ and (b) CD8+ transduced T cells to determine transduction efficiency. Cells positive for mCherry were determined to be transduced. Cell surface CAR expression was determined by MYC-tag (GCT02) or FLAG-tag (C2173) labelling. Data are representative of approximately 5 experiments.

Supplementary Figure 10

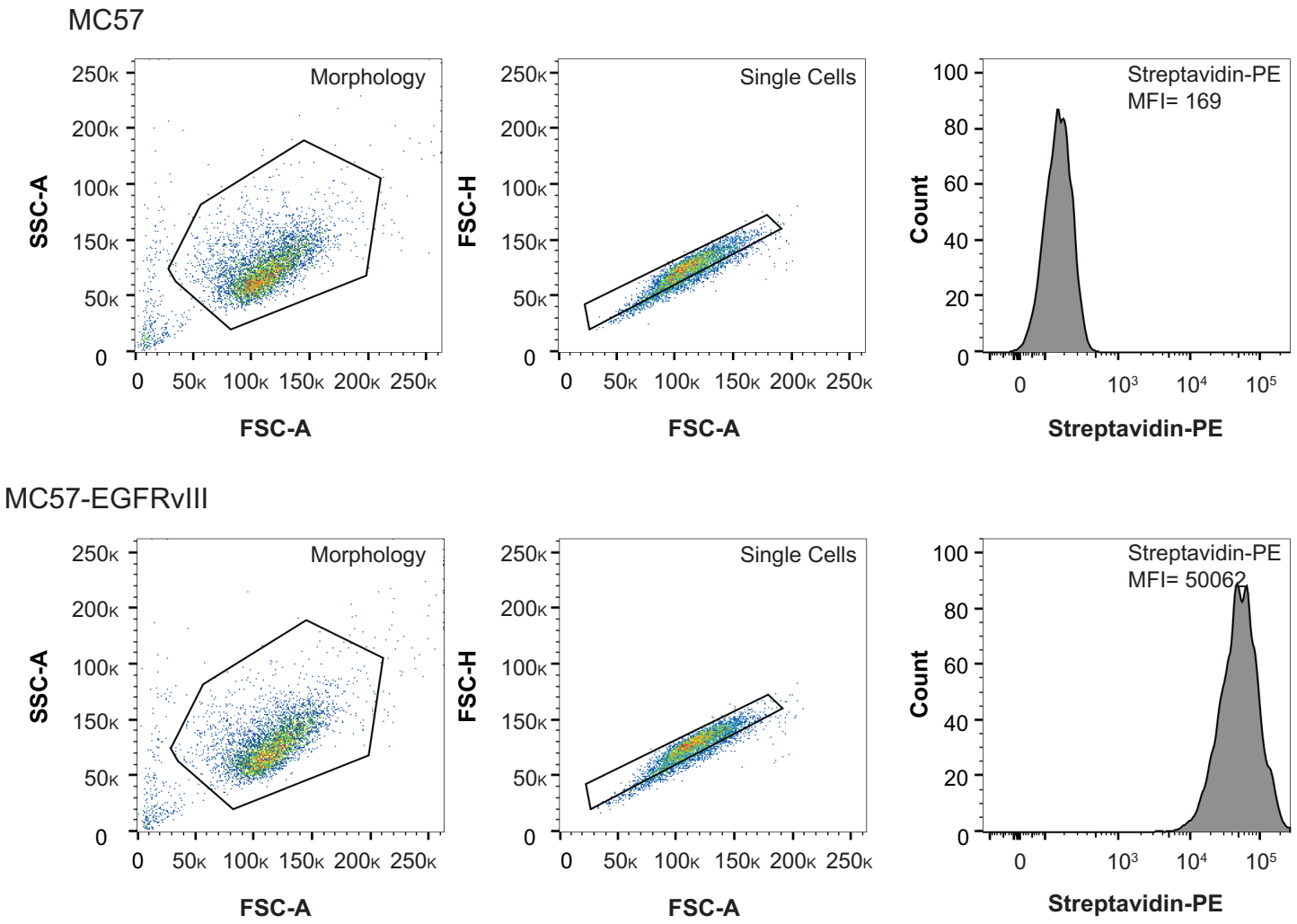

Supplementary Figure 10. Flow cytometry gating strategy for Figure 2f.
(a) Flow cytometry gating strategy of MC57 (top) and MC57-EGFRvIII (bottom) to determine level of GCT02 scFv binding. Data are representative of 3 experiments.

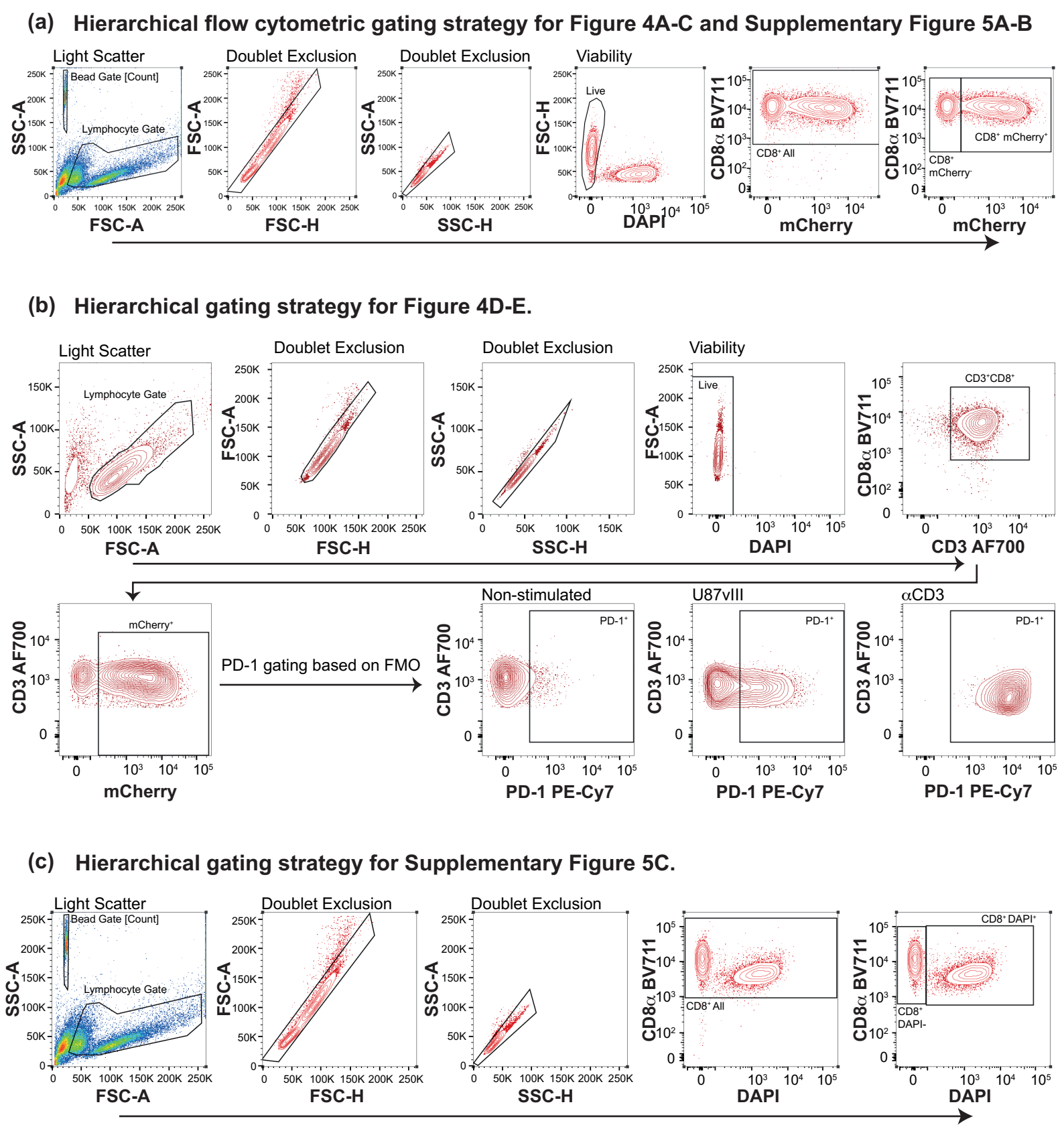

Supplementary Figure 11: Flow cytometry gating strategies for Figure 4a-e and Supplementary Figure 5a-c.

(a-c) Arrows indicate direction of hierarchical gating. **(a)** Counting beads (far left panel) and singlet live CD8⁺ mCherry$^{+/-}$ events (far right panel) identified. Bead counts and CD8⁺ mCherry$^{+/-}$ counts (Figure 4c) and frequencies (Figure 4a-b; Supplementary Figure 5a;c) used for data generation. **(b)** Singlet live CD3⁺ CD8⁺ mCherry⁺ events identified. Within this population PD-1 expression frequency (Figure 4d) and median fluororescence intensity (MFI, Figure 4e) determined by gating based on FMO control. Representative examples of PD-1 staining on: non-stimulated; U87vIII cocultured; and αCD3-stimulated cells (bottom right panels as labelled) shown (Figure 4d-e). **(c)** Counting beads (far left panel) and singlet CD8⁺ live (DAPI⁻) and dead (DAPI⁺) events (far right panel) identified. Bead counts and CD8⁺ DAPI⁺ counts (Supplementary Figure 5b) used for data generation.

Hierarchical gating strategy for Figure 7a-c; e; g-h and Supplementary Figure 7a-c.

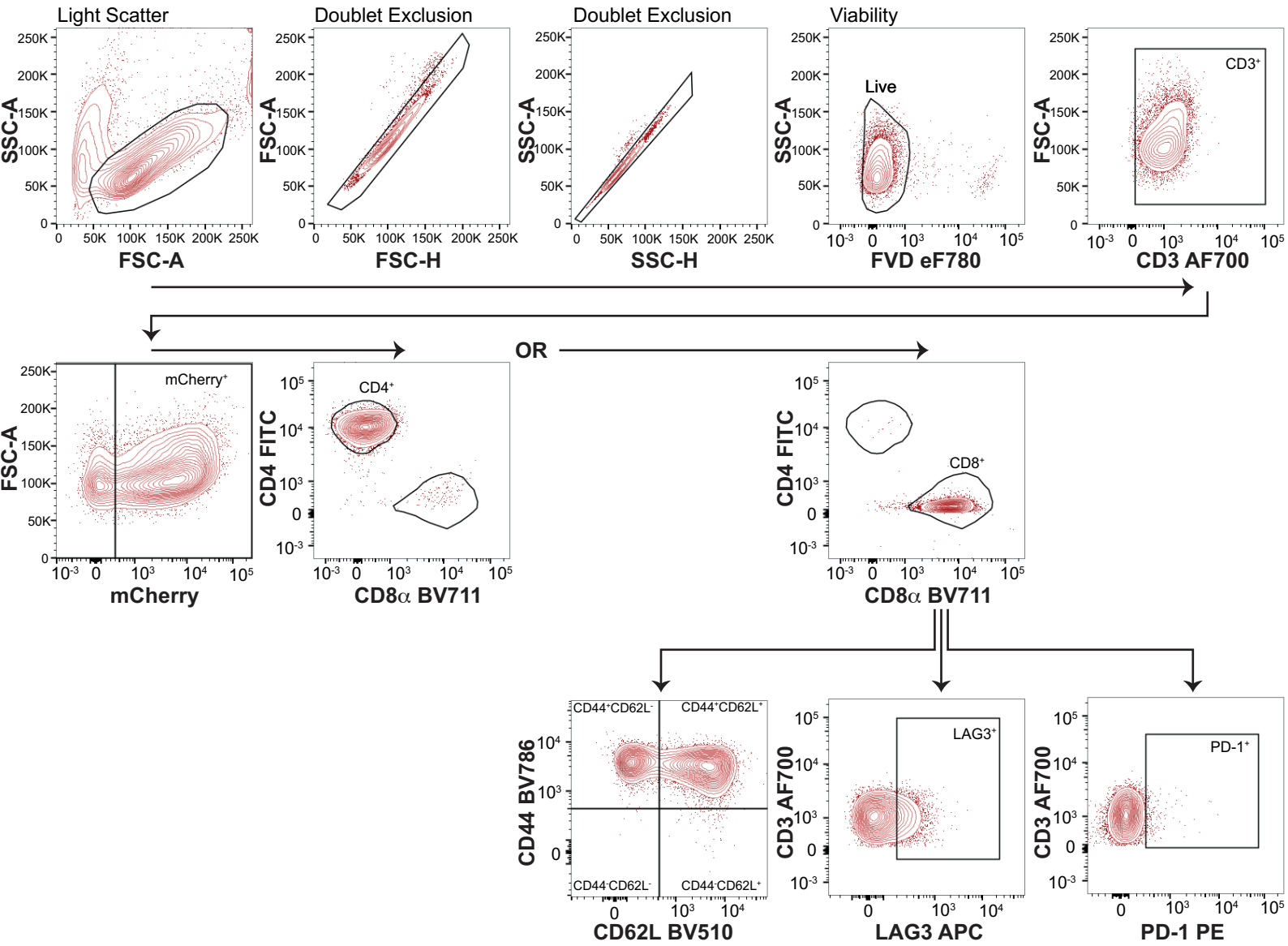

Supplementary Figure 12: Hierarchical gating strategy for immunophenotyping (*in vitro* samples) - Figure 7a-c; e; g-h and Supplementary Figure 7a-c.

Arrows indicate direction of hierarchical gating. Singlet live events were identified by light scatter and fixable viability dye (FVD) exclusion. Within all live events $CD3^+mCherry^+CD4^+$ and $CD3^+mCherry^+CD8^+$ cells were identified. CD44/CD62L coexpression patterns (Figure 7a-b), PD-1 expression frequency (Figure 7c;e) and LAG3 expression frequency (Figure 7g-h) were determined on $CD3^+mCherry^+CD4^+$ and $CD3^+mCherry^+CD8^+$ cells with gating based on CD44, CD62L, PD-1 and LAG3 FMO controls. One representative sample shown.

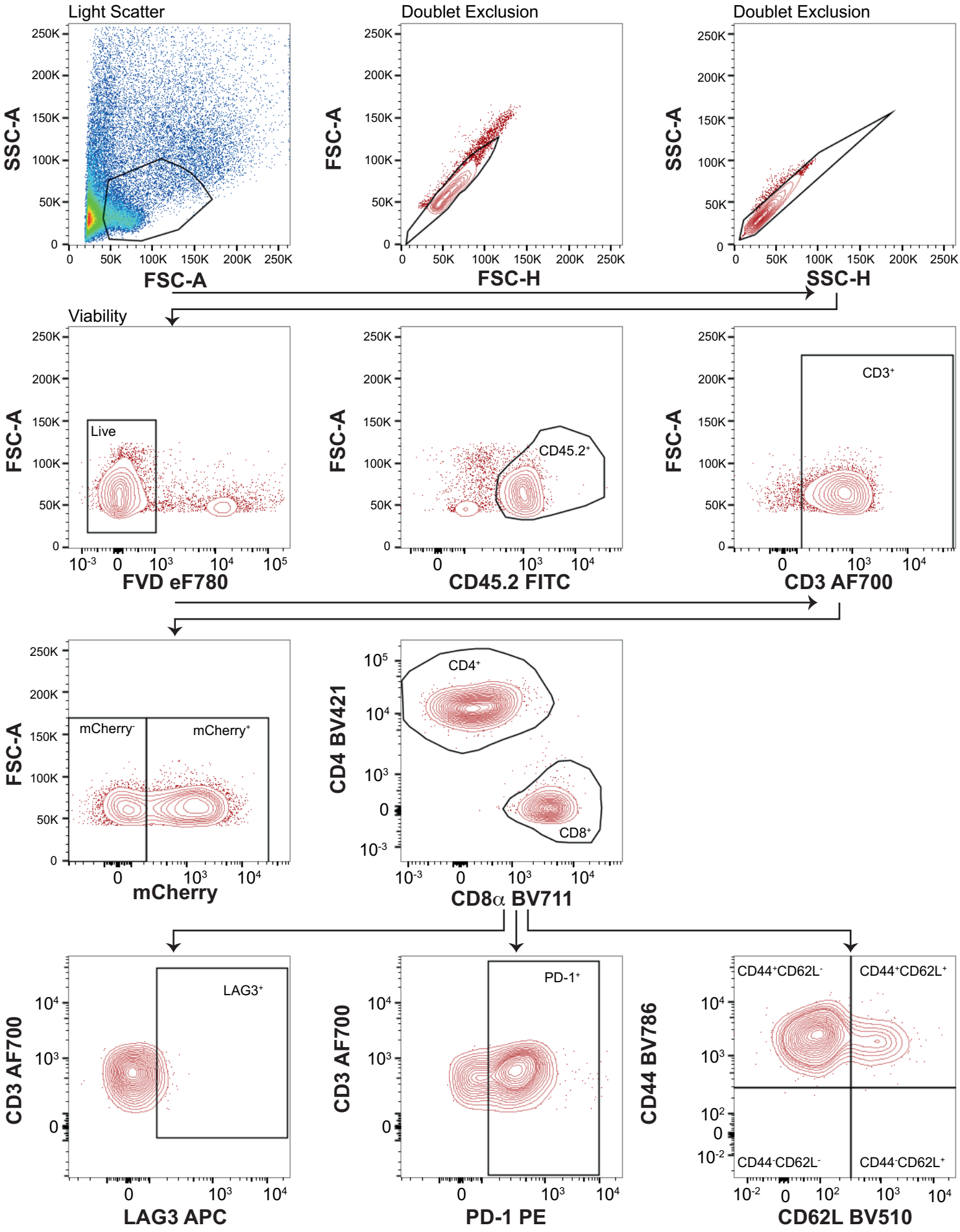

Supplementary Figure 13: Hierarchical gating strategy for immunophenotyping (*ex vivo* samples) - Figure 7a-h and Supplementary Figure 7a-c.

Arrows indicate direction of hierarchical gating. Singlet live events were identified by light scatter and fixable viability dye (FVD) exclusion. Within all live events $CD45.2^{+}CD3^{+}mCherry^{+}CD4^{+}$ and $CD45.2^{+}CD3^{+}mCherry^{+}CD8^{+}$ cells were identified. CD44/CD62L coexpression patterns (Figure 7a-b), PD-1 expression frequency (Figure 7c;e) and MFI (Figure 7d;f), LAG3 expression frequency (Figure 7g-h) and relative $mCherry^{+}CD4^{+}$:$CD8^{+}$ frequencies (Supplementary Figure 7a-c) were determined with gating based on CD44, CD62L, PD-1 and LAG3 FMO controls. One representative spleen sample shown.